BIOCHEMICAL PHARMACOLOGY 72 (2006) 344–357

available at www.sciencedirect.com

SCIENCE DIRECT®

journal homepage: www.elsevier.com/locate/biochempharm

Kinetic analysis of the protection afforded by reversible inhibitors against irreversible inhibition of acetylcholinesterase by highly toxic organophosphorus compounds

Saskia Eckert [a], *Peter Eyer* [a,*], *Harald Mückter* [a], *Franz Worek* [b]

[a] *Walther-Straub-Institute of Pharmacology and Toxicology, Ludwig-Maximilians-University of Munich, Goethestr. 33, D-80336 Munich, Germany*

[b] *Bundeswehr Institute of Pharmacology and Toxicology, Neuherbergstr. 11, D-80937 Munich, Germany*

ARTICLE INFO

Article history:
Received 16 February 2006
Accepted 7 April 2006

Keywords:
Carbamate prophylaxis
Organophosphorus compounds
Acetylcholinesterase
Pyridostigmine
Physostigmine
Huperzine A
Kinetic analysis
Computer simulation

Abbreviations:
AChE, acetylcholinesterase (EC 3.1.1.7)
AU, absorbance units
DTNB, 5,5′-dithiobis (2-nitrobenzoic acid)
HI 6, 1-[[[4-(aminocarbonyl)-pyridinio]methoxy]methyl]-2-[(hydroxyimino)methyl] pyridinium dichloride

ABSTRACT

In organophosphate poisoning, the underlying mechanism of the therapeutic efficacy of carbamate prophylaxis, which was successfully tested in animal experiments, still awaits complete understanding. In particular, it is unclear whether survival is improved by increased acetylcholinesterase activity during the acute phase, when both carbamate and organophosphate are present. This question should be solved experimentally by means of a dynamically working in vitro model. Immobilized human erythrocytes were continuously perfused while acetylcholinesterase activity was monitored in real-time by a modified Ellman method. The concentrations of reversible inhibitors and of paraoxon were varied to assess the influence of both components on the enzyme activity under steady-state conditions. Physostigmine, pyridostigmine and huperzine A were tested for their prophylactic potential. Upon pretreatment with these reversible inhibitors the enzyme was inhibited by 20–90%. Additional perfusion with 1 μM paraoxon for 30 min resulted in a residual activity of 1–4%, at low and high pre-inhibition, respectively. The residual activity was significantly higher than in the absence of reversibly blocking agents (0.3%). After discontinuing paraoxon, the activity increased even in the presence of the reversible blockers. Stopping the reversibly blocking agents resulted in 10–35% recovery of the enzyme activity, depending on the degree of pre-inhibition. The experimental results agreed with computer simulations upon feeding with the essential reaction rate constants, showing that physostigmine was somewhat superior to pyridostigmine in enhancing residual activity in the presence of 1 μM paraoxon for 30 min. The model predicts that inhibitors with a faster dissociation rate, e.g. huperzine A, may be superior in case of a 'hit-and-run' poison such as soman.

* *Corresponding author*. Tel.: +49 89 218075 702; fax: +49 89 218075 701.
E-mail address: peter.eyer@lrz.uni-muenchen.de (P. Eyer).

0006-2952/$ – see front matter © 2006 Elsevier Inc. All rights reserved.
doi:10.1016/j.bcp.2006.04.015

HLö 7, 1-[[[4-(aminocarbonyl)-pyridinio]methoxy]methyl]-2,4-bis[(hydroxyimino)methyl]pyridinium dimethanesulfonate
Hup A, (−)-huperzine A
Physo, (−)-physostigmine
Pyr, pyridostigmine
Px, paraoxon
RBC, red blood cell
TMB-4, (1,1′-trimethylene bis[4-(hydroxyimino)methyl] pyridinium dibromide

1. Introduction

Highly toxic organophosphorus compounds, such as 'nerve agents', are a persistent threat in military conflicts [1] and terrorist attacks [2]. The main toxic action of these agents is generally regarded to result from rapid phosphylation of the catalytic center of acetylcholinesterase (AChE; EC 3.1.1.7), thereby inhibiting hydrolysis of the transmitter acetylcholine and hence disturbing cholinergic transmission. Standard medical treatment includes terminating the exposure, ventilatory support, therapy with a muscarine antagonist and a reactivating oxime [3]. The latter component is effective in sarin and VX poisoning, less effective in tabun and quite ineffective in soman poisoning due to rapid 'aging' of the inhibited AChE. This aging phenomenon results from rapid hydrolysis of the phosphonylated active site serine with the release of pinacolyl alcohol [4]. The ensuing negatively charged residue presumably repels the negatively charged oximate anion and becomes resistant towards its nucleophilic attack [5]. This enzyme species is considered as irreversibly inhibited. Since several amino acid residues surrounding the active center facilitate this aging reaction [6], the observed species differences in the aging half-life [7] became plausible. Unfortunately, primates exhibit particularly short aging half-lives in the range of 1–2 min. Hence, the useful time for effective oxime administration is very short in soman poisoning of humans. In practice, intramuscular injection by autoinjectors in self- or buddy-aid will not produce effective systemic concentrations in less than a few minutes. In fact, the mean absorption half-life of the most advanced reactivator, HI 6 dichloride, was 4 min in healthy volunteers [8]. Similar results were obtained in swine, regardless of the HI 6 salt (dichloride or dimethansulfonate) used [9]. Hence, oxime treatment, even if effective in vitro, probably comes too late in realistic scenarios of soman poisoning.

In the early sixties, when the soman threat and the inability of proper treatment were recognized during the Cold War, other strategies were searched for. Studying the dealkylation mechanism for aging of AChE inhibited by soman, Fleisher and Harris [4] detected that pretreatment with physostigmine elevated the LD50 of soman 3.8 times in atropine-protected rats and enhanced the residual cholinesterase activity of the rat brain. Koster [10] and Koelle [11], in 1946, have already reported that physostigmine protected cholinesterase from irreversible inhibition by diisopropylfluorophosphate. A more systematic study by Berry and Davies [12] revealed that a sign-free dose of physostigmine, when given to guinea-pigs together with atropine before poisoning, raised the LD50 of soman seven to eight times, while atropine or physostigmine alone provided a factor of only 1.5 and 1.8, respectively.

In those days, the antidotal action of reversible cholinesterase inhibitors were referred to their common property of being able to inhibit AChE reversibly and protect the enzyme from irreversible phosphylation. Provided that the absorbed organophosphorus compound was rapidly eliminated, free enzyme would be gradually regenerated to allow survival. The enhancement of protection by atropine was explained by the anti-muscarinic effect during the critical period of otherwise lethal acetylcholine accumulation when both inhibitors were present.

Other carbamates [13–15] and non-acylating inhibitors, such as huperzine, have been successfully tested [16,17] and it turned out that marked species differences existed in the protective ratio that could be afforded by the reversible AChE inhibitors, with mice and rats being less responsive compared to guinea-pigs and non-human primates [12,13,18]. These results may have promoted the guinea-pig model as particularly predictive for man [19]. The enigmatic species difference was plausibly explained later on when the widely varying amounts of carboxylesterase (EC 3.3.1.1) among these species were taken into account. In fact, when protection was expressed as the difference in the soman LD50 values between carbamate-protected animals and control animals, this difference was quite uniform across species. In line with this, pre-inhibition of carboxylesterase by a specific inhibitor, CBDP (2-/o-cresyl/4H:1:3:2-benzodioxaphosphorin-2-oxide), abolished the species difference [20]. Since human plasma does not contain carboxylesterase [21], the scavenging function of patrolling carboxylesterase as observed in mice and rats is lacking.

While these studies indicated beneficial effects of pre-treatment with reversible inhibitors, the mechanism of action still awaited proof. In most studies, 24 h survival was used as an end-point, which gives no information what happens in the early phase when both inhibitors are present. AChE activity was rarely measured at the onset of intoxication (usually within 2 min) and in cases when AChE activity was reported methods for preventing spontaneous reactivation during work-up were not presented. Guinea-pigs challenged with VX and treated with atropine 1 min later had about 3 and 5% of

red blood cell (RBC) AChE activity after saline or pyridostigmine pretreatment, respectively [22]. Since AChE was determined radiometrically, which usually lasts several minutes, spontaneous reactivation during measurement may have obscured the result. In a study with rhesus monkeys [23], oral pyridostigmine pretreatment and therapy with atropine, benactyzine and the oxime TMB-4 saved the animals when exposed up to 10 LD50 soman. In the absence of pyridostigmine pretreatment, the therapeutic cocktail was not superior to atropine alone, which allowed survival from an exposure of soman not greater than two LD50. Pretreatment resulted in 50% RBC–AChE inhibition and a drop to 2.5% of residual activity following soman. Immediately after the onset of toxic signs, the antidotal cocktail was administered and RBC–AChE activity determined some 30 min later showing an increase to about 8% of normal. Unfortunately, no data on work-up of RBCs were given, and it cannot be decided whether the increase of RBC–AChE activity resulted from reactivation by TMB-4 or from decarbamylation only. This reservation regarding residual enzyme activity stems from the fact that decarbamylation half-lives in the range of 15–30 min (37 °C) result in 5% active enzyme within 1.1 and 2.2 min, respectively, a time that will almost always elapse when performing the usual enzyme assays [24]. To conclude, the paucity of experimental proof with regard to the mechanism of carbamate protection during the early phase of intoxication left us somewhat uncomfortable. In addition, also other targets for physostigmine and other carbamates have been proposed, such as direct interactions with the nicotinergic receptor ion channel complex [25].

It thus appeared timely to scrutinize the time course of AChE activity during organophosphate exposure and the influence of pretreatment with reversible AChE inhibitors. To follow minute changes in residual AChE activity in real-time we adopted the perfusion model using human RBC–AChE as presented in the preceding paper. With this tool at hand, we addressed to the following questions: (i) Does pretreatment with a reversible inhibitor result in a higher AChE activity during the presence of an irreversible inhibitor compared to non-pretreatment? (ii) Are there differences in effectiveness among the reversible inhibitors in enhancing residual activity? (iii) Can we define optimal properties of a reversible inhibitor that apply for all intoxication scenarios? We think that the resolution of these questions may be helpful to design and refine animal experiments with the scope to get more insight into the mechanism(s) of beneficial action elicited by the 'carbamate pretreatment'. For the sake of simplicity, we use the term ''reversible'' inhibitors also for the carbamates, knowing that the reaction is not truly reversible since the carbamate is not recovered unchanged.

2. Materials and methods

Customary chemicals were obtained from commercial sources at the purest grade available.

Paraoxon-ethyl and paraoxon-methyl were from Dr. Ehrenstorfer GmbH (Augsburg, Germany). Paraoxon-ethyl was freed from disturbing *p*-nitrophenol as described in the preceding paper. (−)-Physostigmine (eserine hemisulfate) and pyridostigmine bromide were purchased from Sigma (Deisenhofen, Germany), (−)-huperzine A from Calbiochem-Merck (Darmstadt, Germany).

Particle filters employed were Millex®-GS, 0.22 μM (Millipore, Eschborn, Germany).

2.1. General experimental procedure

Experimental procedure was performed as described in the preceding paper using the dynamic model. In short, human erythrocytes were layered onto a particle filter (Millex®-GS, 0.22 μM, Ø33 mm) resulting in a stable enzyme reactor. For

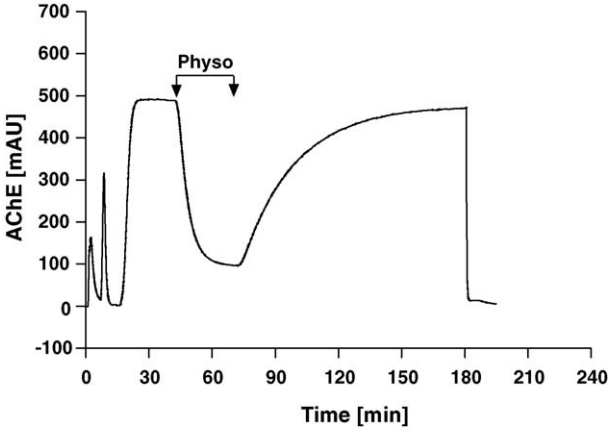

Fig. 1 – Time course of human erythrocyte AChE activity after inhibition with physostigmine (250 nM) and spontaneous reactivation. After inserting the enzyme reactor, perfusion started with gelatin buffer for 5 min, followed by a 5 min water pulse to ensure total hemolysis, before maximum activity was determined upon perfusion with substrate (0.45 mM) and chromogen (0.3 mM). Following the equilibration phase, the enzyme was inhibited with physostigmine. When physostigmine was discontinued, spontaneous reactivation started and the enzyme activity recovered to a maximum value. After 180 min, the enzyme reactor was replaced by a plain filter and the blank values of the complete perfusion medium and gelatin buffer only were determined.

Table 1 – Rate constants of inhibition ($k_{i\ obs}$) and of spontaneous reactivation ($k_{d\ obs}$) of human erythrocyte AChE following inhibition with physostigmine

Physostigmine [nM]	$k_{i\ obs}$ [min^{-1}]	$k_{d\ obs}$ [min^{-1}]
2000	1.013	0.0376
1000	0.670	0.0392
500	0.400	0.0410
250	0.215	0.0408
100	0.115	0.0409
50	0.077	0.0417
25	n.d.	0.0415

The data are means of two to five experiments per concentration; substrate concentration 0.45 mM; the goodness of fit of the individual curves was $R^2 > 0.999$; n.d., not determined.

Table 2 – Rate constants of inhibition ($k_{i\ obs}$) and of spontaneous reactivation ($k_{d\ obs}$) of human erythrocyte AChE following inhibition with pyridostigmine

Pyridostigmine [nM]	$k_{i\ obs}$ [min^{-1}]	$k_{d\ obs}$ [min^{-1}]
5000	0.198	0.0257
2000	0.110	0.0253
1000	0.063	0.0259
500	0.034	0.0260
250	0.030	0.0252

The data are means of one to three experiments per concentration; substrate concentration 0.45 mM; the goodness of fit of the individual curves was $R^2 > 0.997$.

determination of maximum AChE activity the enzyme reactor was continually perfused at 37 °C with the medium, consisting of acetylthiocholine (0.45 mM), DTNB (Ellman's reagent, 0.3 mM), and phosphate buffer (0.1 M, pH 7.4) containing 0.2% (w/v) gelatin. The total flow rate through the enzyme reactor was 0.5 mL/min. The effluent passed a photometer set at 470 nm and digitized absorbance values were collected at 1.6 s intervals. The enzyme reactor was inserted at $t = 0$ and flushed with buffer for 5 min, followed by a pulse of distilled water ($t = 5$) for 5 min and further flushing with buffer ($t = 10$) for 5 min. At $t = 15$, DTNB and acetylthiocholine were added for the determination of the maximum enzyme activity ($t = 30$).

2.2. *Inhibition of AChE with reversible AChE inhibitors and spontaneous reactivation*

Starting at maximum enzyme activity ($t = 30$), AChE was inhibited with different reversible inhibitors at various concentrations until steady state was reached. Inhibition levels at steady state ranged from about 20 to 95%. Upon discontinuation of the reversible inhibitors, spontaneous reactivation started and the enzyme activity recovered to maximum activity.

2.3. *Inhibition of AChE with paraoxon following pre-inhibition with reversible AChE inhibitors*

Following steady-state conditions in the presence of reversible inhibitors ($t = 60$), paraoxon (1 μM) was added for 30 min and residual activity determined ($t = 90$). Paraoxon was discontinued first ($t = 90$) as were the reversible inhibitors 10 min later, before spontaneous reactivation started.

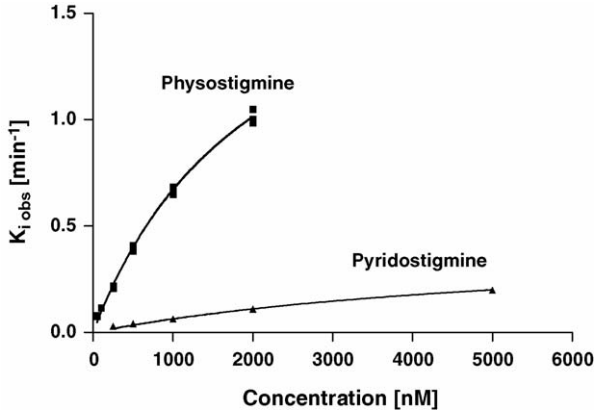

Fig. 2 – Rates of inhibition $k_{i\ obs}$ vs. carbamate concentration in the presence of 0.45 mM acetylthiocholine: (■) physostigmine; (▲) pyridostigmine.

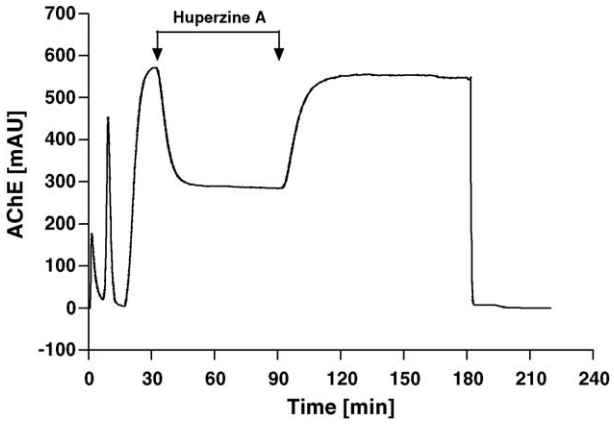

Fig. 3 – Time course of human erythrocyte AChE activity after inhibition with huperzine A (50 nM) and spontaneous reactivation. After attaining the maximal activity, the enzyme was inhibited with huperzine A. When huperzine A was discontinued spontaneous reactivation started and the enzyme activity recovered to a maximum value. After 180 min, the enzyme reactor was replaced by a plain filter and the blank values of the complete perfusion medium and gelatin buffer only were determined.

2.4. *Determination of the non-enzymatic blank value*

After inhibition and reactivation of AChE, the enzyme reactor was replaced by a dummy filter without enzyme source. The blank values of the complete perfusion medium (acetylthiocholine, DTNB and gelatin buffer) and of buffer only were determined. For calculation of residual activity the blank value was subtracted from the levels of inhibition and of maximum activity.

2.5. *Calculations and statistics*

Processing of experimental data is described in the preceding paper. Briefly, absorbance data collected at 1.6 s intervals were analyzed by curve fitting programs provided by Prism™ Version 3.0 (GraphPad Software, San Diego, CA).

Steady-state conditions were assumed when the optical changes were <0.5 mAU/min. Inhibition and reactivation rates were calculated by fitting a mono-exponential decay function and a mono-exponential association function, respectively, to the data points. First-order kinetics were assumed when the goodness of fit exceeded $R^2 = 0.995$. Means are presented along with standard deviation (S.D.) and the number of experiments. Analysis of significance of residual activity in the presence and absence of short-acting inhibitors was performed with the two-tailed Mann–Whitney test provided by Prism™ Version 3.0.

Computer calculations for the simulation of dynamic changes of AChE activities were performed with the software

Table 3 – Rate constants of spontaneous reactivation and inhibition of human erythrocyte AChE following huperzine A

Huperzine A [nM]	$k_{d\ obs}$ [min^{-1}]	$AChE_{max}$ [mAU]	$AChE_{Plateau}$ [mAU]	BV [mAU]	$k_{i\ obs}$ [min^{-1}]
1000	0.076	521.5	24.9	6.1	2.016
500	0.113	541.4	46.3	6.9	1.425
250	0.129	538.2	78.2	7.2	0.836
100	0.143	564.4	168.8	8.0	0.352
100	0.144	547.4	159.6	8.1	0.370
50	0.141	533.1	221.6	7.6	0.206
50	0.147	489.8	204.7	7.1	0.212
25	0.159	531.6	314.8	6.5	0.112
25	0.154	602.0	367.2	6.9	0.101
10	0.153	464.0	361.5	6.1	0.044

R^2 (quality of curve fitting) was >0.996 for the determination of $k_{d\ obs}$; $AChE_{max}$ is the maximum enzyme activity, $AChE_{Plateau}$ the enzyme activity at steady state and BV is the blank value of the complete perfusion medium. The rate constants $k_{i\ obs}$ of inhibition with huperzine A were calculated from the equilibrium attained and the spontaneous reactivation according to ref. [24]; substrate concentration was 0.45 mM.

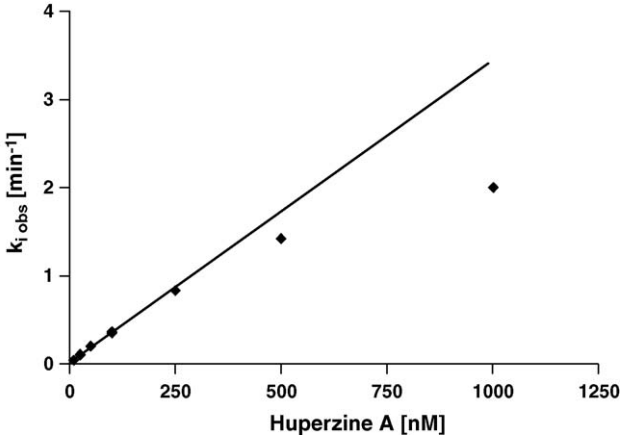

Fig. 4 – Rate of inhibition $k_{i\ obs}$ depending on huperzine A concentration in the presence of 0.45 mM acetylthiocholine.

Maple 9.0 (Maplesoft, Waterloo, Canada) by solving numerically multiple differential equations (basics are detailed in ref. [26]).

For curve simulations (see Section 4), the following kinetic data were applied: inhibition rate constant of paraoxon $k_{i\ obs} = 0.279\ min^{-1}$ for 1 μM paraoxon (cf. preceding paper). The inhibition rate constant for huperzine A $k_{i\ obs}$ was calculated according to [24]:

$$k_{i\,obs} = \frac{k_{d\,obs} \times (AChE_{max} - AChE_{plateau})}{AChE_{plateau} - BV}$$

For huperzine A, the values of $k_{i\ obs}$ shown in Table 3 were used as 'k_c' (see Section 4).

3. Results

3.1. *Inhibition of AChE with reversible AChE inhibitors and spontaneous reactivation*

Fig. 1 shows the AChE activity of human erythrocyte ghosts versus time and the influence of physostigmine. Following insertion of the loaded filter a short-lasting peak, indicating the disequilibrium of the system, was followed by a higher peak due to hemolysis of RBCs upon a short pulse with distilled water. When DTNB and the substrate acetylthiocholine were included the absorbance rose to about 500 mAU and remained at that level until physostigmine, 250 nM, was added. The absorbance gradually dropped in a mono-exponential manner until a new equilibrium was reached at some 100 mAU. When physostigmine was discontinued the activity recovered to about 95% of the initial activity. After 180 min, the filter was removed to establish the reagent blank value (DTNB and acetylthiocholine) before the buffer blank returned to the starting value. Analysis of the inhibition and decarbamylation reaction course allowed the establishment of the kinetic constants. Both reactions followed a mono-exponential function. In the presence of 0.45 mM substrate, the observed k_i values for inhibition and k_d values for decarbamylation are presented in Table 1.

The influence of pyridostigmine was tested in a similar manner with the results shown in Table 2. The half-lives for return of activity were 16.9 ± 0.3 min (n = 17; 25–500 nM) for physostigmine and 27.0 ± 0.8 min (n = 9; 250–5000 nM) for pyridostigmine. The dependence of the observed inhibition

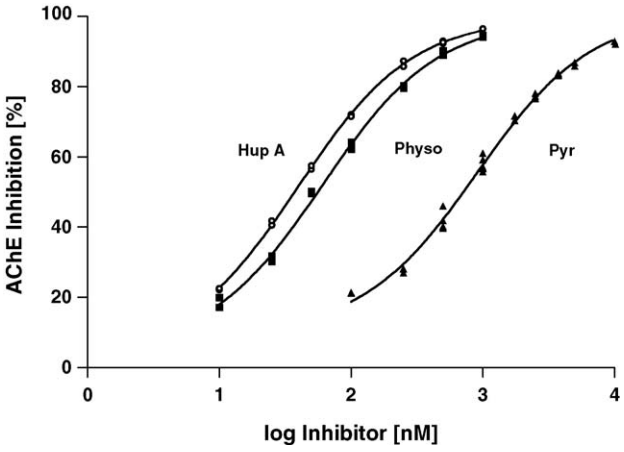

Fig. 5 – AChE inhibition by huperzine A, physostigmine and pyridostigmine. IC_{50} values were calculated from sigmoidal concentration vs. inhibition curves with Hill n = 1. IC_{50} ± S.D. (n; R^2 goodness of fit): huperzine A, 40 ± 1 nM (16; 0.999); physostigmine, 61 ± 3 nM (23; 0.997); pyridostigmine, 904 ± 60 nM (27; 0.995).

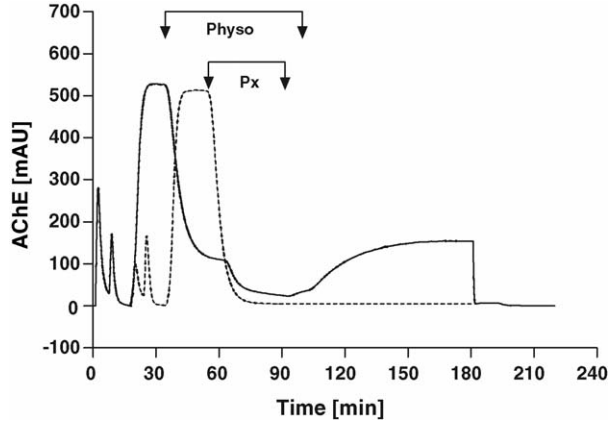

Fig. 6 – Time course of human erythrocyte AChE activity after inhibition with physostigmine and paraoxon (solid line), in comparison to inhibition with paraoxon alone (dotted line). After attaining the maximal activity, the enzyme was inhibited with physostigmine (250 nM) for 30 min, followed by 30 min of both physostigmine (250 nM) and paraoxon (1 μM). After simultaneous perfusion, paraoxon was discontinued first and perfusion with physostigmine only continued for 10 min. Then, physostigmine was also stopped and spontaneous reactivation started. The enzyme activity recovered to a maximum value. After 180 min, the enzyme reactor was replaced by a plain filter and the blank values of the complete perfusion medium and gelatin buffer only were determined.

rate constants on the carbamate concentration is depicted in Fig. 2. These data suggested that there is no linear increase of the observed inhibition rate constants on the carbamate concentration in the range investigated. Rather, a Michaelis-type behavior is apparent, pointing to a saturation phenomenon. In fact, a rectangular hyperbola closely fitted the experimental data.

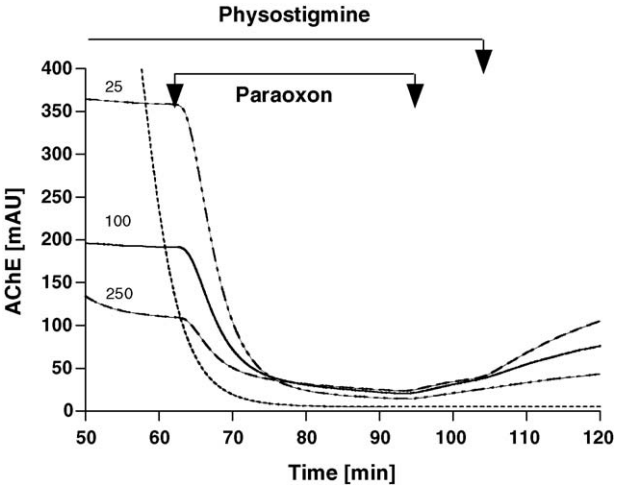

Fig. 7 – Time course of human erythrocyte AChE activity after inhibition with various concentrations of physostigmine and paraoxon, in comparison to inhibition with paraoxon alone (dotted line). Physostigmine concentrations (nM) as indicated, paraoxon (1 μM); for further details, see Fig. 6.

In contrast to the carbamates, huperzine A is considered a non-acylating, reversible inhibitor of AChE [27]. Fig. 3 shows the fast inhibition by huperzine A and the fast reactivation of the inhibited enzyme. After discontinuation of huperzine A, 96.5 ± 1.1% ($n = 10$) of the initial activity was reached. Unexpectedly, the spontaneous reactivation was considerably retarded when huperzine A at high concentrations was discontinued (Table 3). We considered this phenomenon a technical artifact due to some leaching of huperzine A from the inevitable dead volumes (see discussion in preceding paper) and only used the values of huperzine A between 10 and 100 nM for further analysis. From this, a mean reactivation half-life of 4.6 ± 0.2 min ($n = 7$; 10–100 nM) was calculated. Due to system-inherent hysteresis, inhibition rates of huperzine A were sometimes too high for our routine analysis (mono-exponential decay function fitted to data). As an alternative, we employed the method of Aldridge and Reiner (Eq. A2.17) [24], which calculates the inhibition rate constant from the ratio of active and inactive enzyme at steady state and from the spontaneous reactivation rate constant. We had expected a linear increase of the observed first-order rate constant of inhibition versus the inhibitor concentration, but found a systematic aberration beyond a huperzine A concentration >100 nM (Fig. 4). The concentration–response curve of the reversible inhibitors with the respective IC_{50} values is shown in Fig. 5.

3.2. *Influence of reversible inhibition of AChE on the residual activity upon paraoxon addition and on the recovery of enzyme activity after discontinuation of both inhibitors*

Fig. 6 shows a typical experiment with physostigmine. After having established the maximal enzyme activity of the reactor, physostigmine (250 nM) was added, which resulted in a residual activity of some 20%. After 60 min, paraoxon (1 μM) was included with physostigmine still being present. Paraoxon rapidly reacted with the free enzyme and – in a slower second phase – with the enzyme regenerated from the carbamylated store. When paraoxon was discontinued at $t = 90$ min, a small increase in activity was observed. Enzyme activity was regenerated more rapidly when also physostigmine was discontinued at $t = 100$ min. A control experiment with paraoxon only (dotted line) showed that the residual activity of AChE was lower in the absence of the carbamate. As shown in the preceding paper, the residual activity of AChE fell to 0.32 ± 0.12% ($n = 13$) upon exposure to 1 μM paraoxon for 33 min. Virtually no reactivation was detected within 30 min upon discontinuation of paraoxon. Calculation indicates that spontaneous reactivation of 0.5% might have occurred (spontaneous reactivation and aging $k = 0.021\ h^{-1}$ each.

Tables 4–6 show the data along with the final AChE activity after discontinuation of the reversible inhibitors. The residual activity in the presence of both reversible inhibitors and paraoxon increased with the extent of pre-inhibition peaking at some 80% pre-inhibition. A typical example for physostigmine is shown in Fig. 7. The residual activity was significantly lower ($p < 0.004$) in the absence of short-acting

Table 4 – Influence of pre-inhibition of AChE on the residual activity in the presence of both physostigmine and paraoxon

Physostigmine [nM]	$AChE_{inhibited}$ physostigmine [%]	$AChE_{inhibited}$ physostigmine + Px [%]	Residual AChE activity [%]	AChE activity after spontaneous reactivation [%]
1000	94.3	96.9	3.1	42.3
1000	94.7	97.3	2.7	42.2
500	89.0	96.5	3.5	35.8
500	90.3	96.6	3.4	35.0
250	79.7	96.3	3.7	27.9
250	80.0	96.4	3.6	28.3
250	80.2	96.3	3.7	29.6
250	80.4	96.3	3.7	28.9
100	62.2	96.7	3.3	20.0
100	62.4	97.0	3.0	19.9
100	62.4	96.7	3.3	20.5
100	63.5	96.8	3.2	20.3
100	64.3	96.9	3.1	19.3
50	50.2	96.9	3.1	14.1
50	49.6	97.2	2.8	13.9
50	49.9	97.4	2.6	13.7
25	30.3	98.1	1.9	10.6
25	31.4	98.2	1.8	10.3
25	30.8	98.1	1.9	10.5
25	31.5	98.1	1.9	11.5
25	31.9	98.3	1.7	10.4
10	20.0	98.5	1.5	5.8
10	17.2	98.7	1.3	6.0

The experiments were performed in the presence of substrate (0.45 mM). When the pre-inhibition by physostigmine at various concentrations had reached steady state, paraoxon (Px, 1 μM) was added for 30 min to determine residual activity. Then, paraoxon was discontinued as was physostigmine 10 min later, resulting in spontaneous reactivation that was determined 80 min later.

Table 5 – Influence of pre-inhibition of AChE on the residual activity in the presence of both pyridostigmine and paraoxon

Pyridostigmine [μM]	$AChE_{inhibited}$ pyridostigmine [%]	$AChE_{inhibited}$ pyridostigmine + Px [%]	Residual AChE activity [%]	AChE activity after spontaneous reactivation [%]
10	92.4	96.5	3.5	31.2
10	92.9	97.1	2.9	39.8
5	85.9	96.8	3.2	35.2
5	86.9	96.6	3.4	31.3
3.75	83.9	97.3	2.7	33.3
3.75	83.2	96.8	3.2	34.0
3.75	83.5	97.0	3.0	33.0
2.5	76.6	97.1	2.9	31.4
2.5	77.3	97.2	2.8	30.2
2.5	78.1	97.4	2.6	29.5
1.75	70.4	97.0	3.0	27.3
1.75	71.7	97.3	2.7	25.9
1	55.8	97.4	2.6	21.3
1	56.7	97.2	2.8	21.2
1	57.1	97.3	2.7	20.9
1	61.0	97.5	2.5	23.3
1	59.2	97.4	2.6	23.1
0.5	46.0	97.5	2.2	–
0.5	40.2	97.9	2.1	15.7
0.5	39.7	98.0	2.0	15.4
0.5	41.9	98.1	1.9	15.7
0.25	28.0	98.5	1.5	12.0
0.25	28.2	98.4	1.6	11.5
0.25	28.0	98.4	1.6	11.6
0.25	27.0	98.5	1.5	12.9
0.1	21.4	99.4	0.6	8.3
0.1	21.2	99.2	0.8	9.7

The experiments were performed in the presence of substrate (0.45 mM). When the pre-inhibition by pyridostigmine had reached steady state, paraoxon (Px, 1 μM) was added for 30 min to determine residual activity. Then, paraoxon was discontinued as was pyridostigmine 10 min later, resulting in spontaneous reactivation that was determined 80 min later.

Table 6 – Influence of pre-inhibition of AChE on the residual activity in the presence of both huperzine A and paraoxon

Huperzine A [nM]	$AChE_{inhibited}$ huperzine A [%]	$AChE_{inhibited}$ huperzine A + Px [%]	Residual AChE activity [%]	AChE activity after spontaneous reactivation [%]
1000	96.5	97.9	2.1	50.8
500	93.0	96.9	3.1	37.2
500	92.6	96.4	3.6	37.7
500	92.4	96.3	3.7	38.7
500	92.7	96.4	3.6	39.2
250	85.8	95.7	4.3	25.5
250	87.4	96.3	3.7	23.7
250	85.8	95.8	4.2	25.5
100	72.1	96.5	3.5	11.4
100	71.5	96.4	3.6	10.7
50	56.5	97.5	2.5	5.5
50	57.5	97.3	2.7	5.4
25	40.6	98.4	1.6	3.8
25	41.9	98.3	1.7	3.7
10	22.2	99.2	0.8	2.6
10	22.6	99.3	0.7	2.5

The experiments were performed in the presence of substrate (0.45 mM). When the pre-inhibition by huperzine A at various concentrations had reached steady state, paraoxon (Px, 1 μM) was added for 30 min to determine residual activity. Then, paraoxon was discontinued as was huperzine A 10 min later, resulting in spontaneous reactivation that was determined 80 min later.

Table 7 – Rate constants k_2, K_d and k_2/K_d of carbamylated human erythrocyte AChE

Carbamate	k_2 (min^{-1})	K_d [μM]	k_2/K_d ($M^{-1}\,min^{-1}$)
Physostigmine ($n = 20$)	2.08 ± 0.10	0.350 ± 0.027	5.94×10^6
Pyridostigmine ($n = 8$)	0.431 ± 0.069	0.979 ± 0.235	0.44×10^6

K_d denotes the dissociation constant of the Michaelis-type complex, k_2 the first-order decay constant of the complex, i.e. the carbamylation constant proper, and k_2/K_d the second-order rate inhibition constant. Data apply for the absence of substrate.

inhibitors than in their presence when >30% of the enzyme was pre-inhibited.

4. Discussion

To the best of our knowledge, this in vitro study shows for the first time that pre-inhibition of AChE by a reversible inhibitor allows a higher proportion of the enzyme to remain active in the presence of an irreversible inhibitor than in the absence of the pretreatment. While preservation of enzyme activity from irreversible phosphylation is the most plausible explanation why the enzyme activity regenerates faster when the irreversible inhibitor has been removed, it is hard to understand why the residual enzyme activity is higher during that phase, when both inhibitors are present together. In fact, it has been reasoned that animal pretreatment with a reversible inhibitor followed by an irreversible one causes a critical period of acetylcholine accumulation when the enzyme is inactivated, both reversibly and irreversibly, needing treatment with atropine [12]. Thus, it remained an enigma why more animals survived the acute phase of poisoning after pretreatment (followed by atropine post poisoning) compared to those animals, which had received atropine only.

In 1983, Albert L. Green [28] presented a 'theoretical kinetic analysis of the protective action exerted by eserine and other carbamate anticholinesterases against poisoning by organophosphorus compounds'. The major conclusion derived thereof was that the protective action of carbamates is essentially prophylactic and does not depend on competition between carbamate and organophosphorus compound for the active site of AChE. Carbamates rather provide a pool of sequestered inactive AChE, which is resistant to phosphylation, but furnishes a steady supply of active enzyme. As a result, Green predicted that a small percentage of active AChE would be present at any time, allowing survival during the very acute phase of poisoning. Interestingly, this originative work was hardly cited and the apparent paradox still awaited experimental proof.

By using the dynamic model (cf. preceding paper), we could mimic the time course of pretreatment followed by

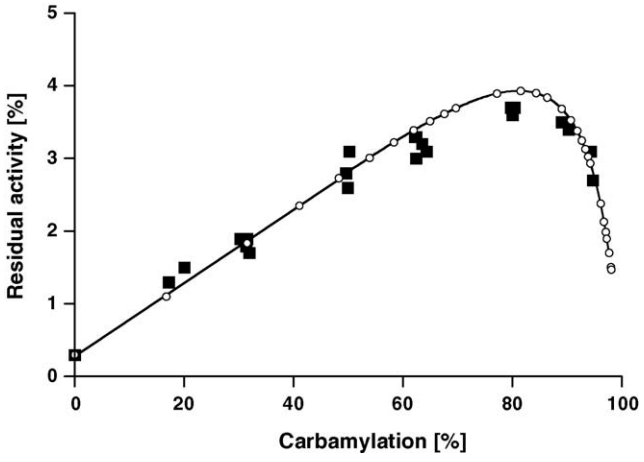

Fig. 8 – Residual AChE activity following simultaneous inhibition with physostigmine and paraoxon (1 μM, 30 min) vs. the degree of pre-inhibition: (■) experimental data; (○) calculated data.

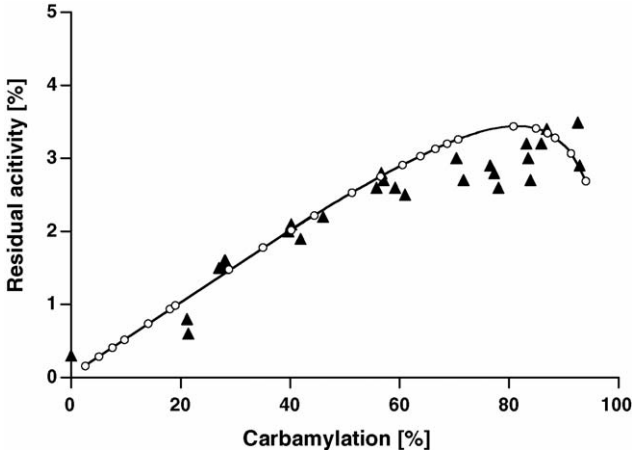

Fig. 9 – Residual AChE activity following simultaneous inhibition with pyridostigmine and paraoxon (1 μM, 30 min) vs. the degree of pre-inhibition: (▲) experimental data; (○) calculated data.

irreversible phosphylation. It was this model that not only allowed continuous AChE activity determination in real-time but also avoided the accumulation of reaction products. Moreover, the model allowed the calculation of the various rate constants that were involved in all the simultaneous reactions. Hence, it was tempting to calculate the course of AChE activity that should result in a defined scenario and to compare the results obtained experimentally for validation of the model.

The simplest model is depicted in Scheme 1:

where E denotes the active enzyme, EC the reversibly inhibited (carbamylated) enzyme and EP the irreversibly inhibited (phosphylated) enzyme; k_d, k_c and k_i indicate the rate constants of spontaneous reactivation (decarbamylation),

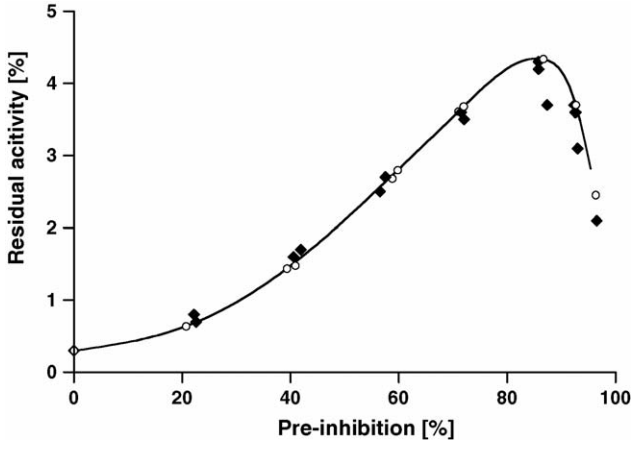

Fig. 10 – Residual AChE activity following simultaneous inhibition with huperzine A and paraoxon (1 μM, 30 min) vs. the degree of pre-inhibition: (◆) experimental data; (○) calculated data.

reversible inhibition (carbamylation) and irreversible inhibition (phosphylation), respectively. For the sake of simplicity, we regard phosphylation by, e.g. paraoxon as irreversible in the time frame of interest, i.e. 30 min at a half-life of 31 h for spontaneous reactivation [29].

The irreversible inhibition rate constant k_i (min^{-1}) was calculated from $k_i = k_p \times [OP]$ for $[OP] \gg [E]$ and disregarding any appreciable built-up of a Michaelis-type complex (dissociation constant, 5–10 μM [30]); k_p denotes the second-order rate constant of phosphorylation and [OP] the organophosphate concentration. The carbamylation rate constant was:

$$k_c = \frac{k_2}{1 + K_d/[\mathrm{Carb}]}, \quad (1)$$

with k_c being the apparent first-order carbamylation rate constant, k_2 the first-order decay constant of the Michaelis-type complex and K_d is the dissociation constant of the Michaelis complex. Since our data were obtained in the presence of substrate, we have to regard the competing substrate acylation reaction. As deduced by Hart and O'Brien [31], only K_d is affected by the competing substrate, but not k_2. Because under the conditions employed the substrate concentration (0.45 mM) was five-fold higher than the Michaelis constant [32], the true K_d value in the absence of substrate is six times lower than that observed in our experiments. The data for physostigmine and pyridostigmine are compiled in Table 7. It should be noted that the parameter k_2/K_d resembles a second-order rate inhibition constant, but has not the same meaning as a bimolecular rate constant [31].

The time-dependent fractional changes of E and EC were calculated by the following differential equations, which were solved numerically using Maple 9.0. The resolution was performed piecewise with $t < t_0$ and $t > t_0$, where t_0 denotes the time point when the OP was added.

$$\frac{d[E]}{dt} = -k_c \times [E] + k_d \times [EC] \quad (\text{for } t < t_0) \quad (2)$$

and

$$\frac{d[E]}{dt} = -k_i \times [E] - k_c \times [E] + k_d \times [EC] \quad (\text{for } t > t_0) \quad (3)$$

and

$$\frac{d[EC]}{dt} = -k_d \times [EC] + k_c \times [E] \quad (4)$$

We calculated k_c for various carbamate concentrations using the experimental parameter $K_{d\ obs} = 6 \times K_d$ (Eq. (1)).

Fig. 8 shows the results observed experimentally (solid squares) and the data calculated by Eqs. (2)–(4) (open circles). The degree of carbamylation at equilibrium is indicated by the *X*-axis. The ordinate shows the residual AChE activity obtained after carbamylation by physostigmine at various concentrations for 60 min followed by 30 min paraoxon (1 μM). The solid curve was drawn to pass through all calculated points without implying a specific analytical function. Interestingly, the linear part of the curve intersects the *Y*-axis at 0.3%, which was the residual activity obtained in the absence of physostigmine. Maximal residual activity (3.9%) was found when about 80% of the enzyme was carbamylated.

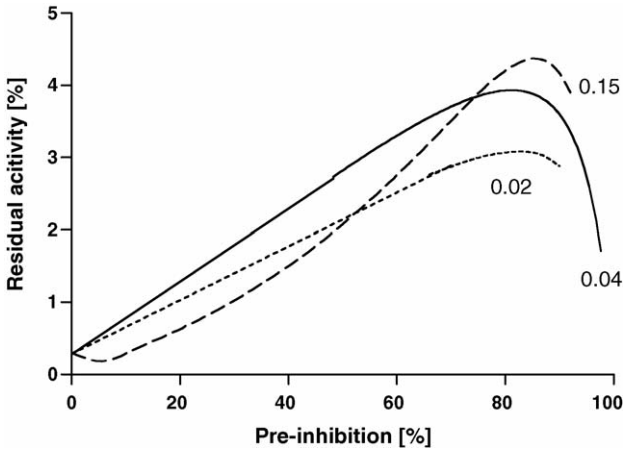

Fig. 11 – Calculated residual activity after 30 min paraoxon (k_i = 0.279 min^{-1}) depending on different degrees of AChE pre-inhibition and various reactivation rate constants k_d (min^{-1}), as found for huperzine A (0.15), physostigmine (0.04) and pyridostigmine (0.02).

Qualitatively similar results were found for pyridostigmine pretreatment (Fig. 9). Again, maximal residual activity (3.4%) is calculated when about 80% of the enzyme is carbamylated, values approximately found in the experiments. A different curve was obtained when huperzine A data were used for calculation (Fig. 10). The linear part of the curve at low pre-inhibition is no longer apparent, while the zenith is again around 80% pre-inhibition with 4.4% residual activity.

These data point to a marked influence of the reactivation rate constant on the residual activity (at constant pre-inhibition level). Fig. 11 shows a plot of the residual activity after 30 min paraoxon (1 μM) versus pre-inhibition level, using various reactivation rate constants (min^{-1}) as indicated. The model predicts that high reactivation rates are of disadvantage

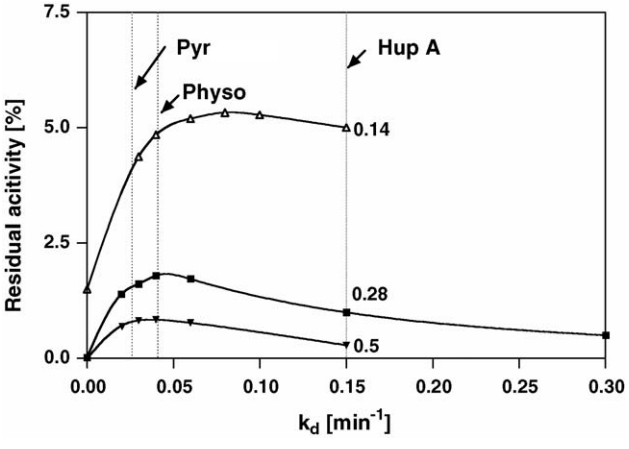

Fig. 12 – Calculated residual activity at 30% pre-inhibition, depending on the reactivation rate constant k_d with varying rate of phosphylation (k_i = 0.14–0.5 min^{-1}; the vertical lines indicate the k_d values for physostigmine (0.041 min^{-1}), pyridostigmine (0.026 min^{-1}) and huperzine A (0.15 min^{-1}), as determined experimentally.

Table 8 – Toxicokinetic data of (P−,C±)soman used for calculation of a simulated scenario

Dose of P(−),C(±)soman	82 nmol/kg
B	71.5 nM
C	4.6 nM
k_{abs}	0.693 min^{-1}
$k_{el\,1}$	0.245 min^{-1}
$k_{el\,2}$	0.05 min^{-1}
k_p	1.5×10^7 M^{-1} min^{-1}
k_a	0.35 min^{-1}

The values of B, C, $k_{el\,1}$ and $k_{el\,2}$ were taken from experiments with marmosets [35], where the biphasic decrease of soman was described by: $[soman]_t = B \times \exp^{-k_{el\,1} \times t} + C \times \exp^{-k_{el\,2} \times t}$. The absorption phase was arbitrarily set to k_{abs} = 0.693 min^{-1}, the phosphylation rate constant k_p was taken from ref. [26] and corrected for the presence of substrate as deduced for the carbamylation rate (see above), k_a is the mean aging rate constant 0.35 min^{-1} [5,47,48]. Spontaneous reactivation was considered insignificant.

at low pre-inhibition levels, whereas high reactivation rates are of advantage at high pre-inhibition levels.

Finally, we looked at the influence of the reactivation rate constant on the residual activity at a fixed level of 30% pre-inhibition, a level which was not associated with significant adverse effects in humans [33] and did not cause interference with performance of a wide range of the most demanding physical and mental tasks [34]. We calculated the data for three different levels of phosphylation rate constants (0.14 min^{-1} corresponds to 0.5 μM paraoxon, 0.28 min^{-1} to 1 μM paraoxon, and 0.5 min^{-1} to 1.8 μM paraoxon, inhibition for 30 min each). The vertical lines in the graph of Fig. 12 indicate the k_d values for pyridostigmine, physostigmine, and huperzine A. It is obvious that a reactivation half-life of some 14 min (k_d = 0.05 min^{-1}) would be optimal, a value that is nearly met by physostigmine (17 min), less by pyridostigmine (27 min) and least by huperzine A (4.6 min).

For the sake of simplicity, the above considerations were initially applied to a constant concentration of the organophosphate over a given time. It was also tempting to simulate more realistic scenarios, e.g. rapid absorption of a poison followed by quick distribution/elimination such as in the case of quick uptake of the 'hit-and-run' poison soman, for which the prophylaxis was primarily designed. The soman concentration profile was calculated as the sum of a Bateman function with rapid absorption (k_{abs}) and rapid distribution/elimination ($k_{el\,1}$) followed by a much slower elimination ($k_{el\,2}$) from a deeper compartment as observed with soman in guinea-pigs and marmosets [35]. To this end, we applied the following simplified equation:

$$[soman]\,(t) = B \times \left[\frac{k_{abs}}{k_{abs} - k_{el\,1}}\right] \times (\exp^{-k_{el\,1} \times t} - \exp^{-k_{abs} \times t}) + C \times \exp^{-k_{el\,2} \times t}$$

The kinetic data were obtained from experiments with atropinized and mechanically ventilated marmosets upon an i.v. challenge with six LD50 soman [35] and were linearly extrapolated to three LD50. All data refer to the toxic stereoisomers of P(−),C(±)soman.

Table 8 shows the values used for the simulation. Pre-inhibition levels (90 min) under steady state were set at 40% and the concentration of the reversible inhibitor was considered constant during and after the soman challenge (90 min). The course of the concentrations of free enzyme (E), the reversibly inhibited enzyme (EC) and the pinacolyl methylphosphonyl enzyme (EP, before aging) was calculated by solving numerically three differential equations as indicated above.

Figs. 13 and 14 (enlarged for the time frame of major interest) show that, in the absence of pretreatment, the enzyme activity is rapidly diminished by soman and the lethal margin of 3% residual activity is reached 6.5 min after challenge. Similarly, EP rapidly decreases due to quick aging. Pretreatment with pyridostigmine results in a nadir of 3.3% of residual activity and in a final increase of 14.9% after 180 min. Similarly, physostigmine achieves a nadir of 4.3% and a final recovery of 13.5%, while pretreatment with huperzine A allows a nadir of 7.7%, an intermediary zenith of 8.4%, but a secondary decrease to 7.0% after 180 min. This latter behavior is remarkable in that it demonstrates that the rapid delivery of active enzyme enables regeneration of sufficient enzyme to keep the nadir quite high, but at the expense of enhanced phosphylation during a phase where soman still resides at

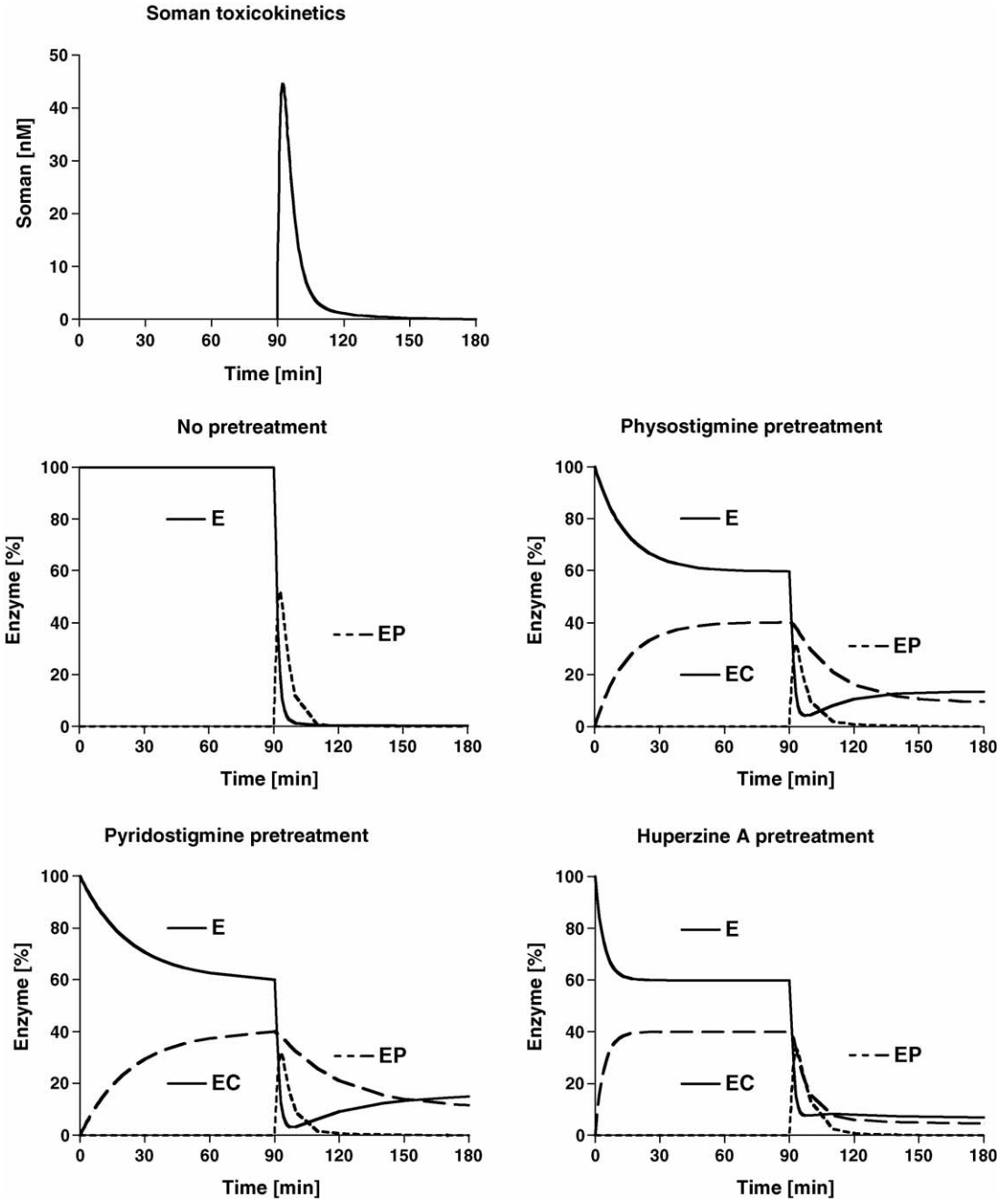

Fig. 13 – Influence of various pretreatment regimes on AChE following soman challenge: E (solid line), active enzyme; EC (dashed line), reversibly inhibited enzyme; EP (dotted line), phosphonylated, unaged enzyme. Following pretreatment with the reversible inhibitor, soman was added after 90 min at the simulated concentration shown in the left upper panel.

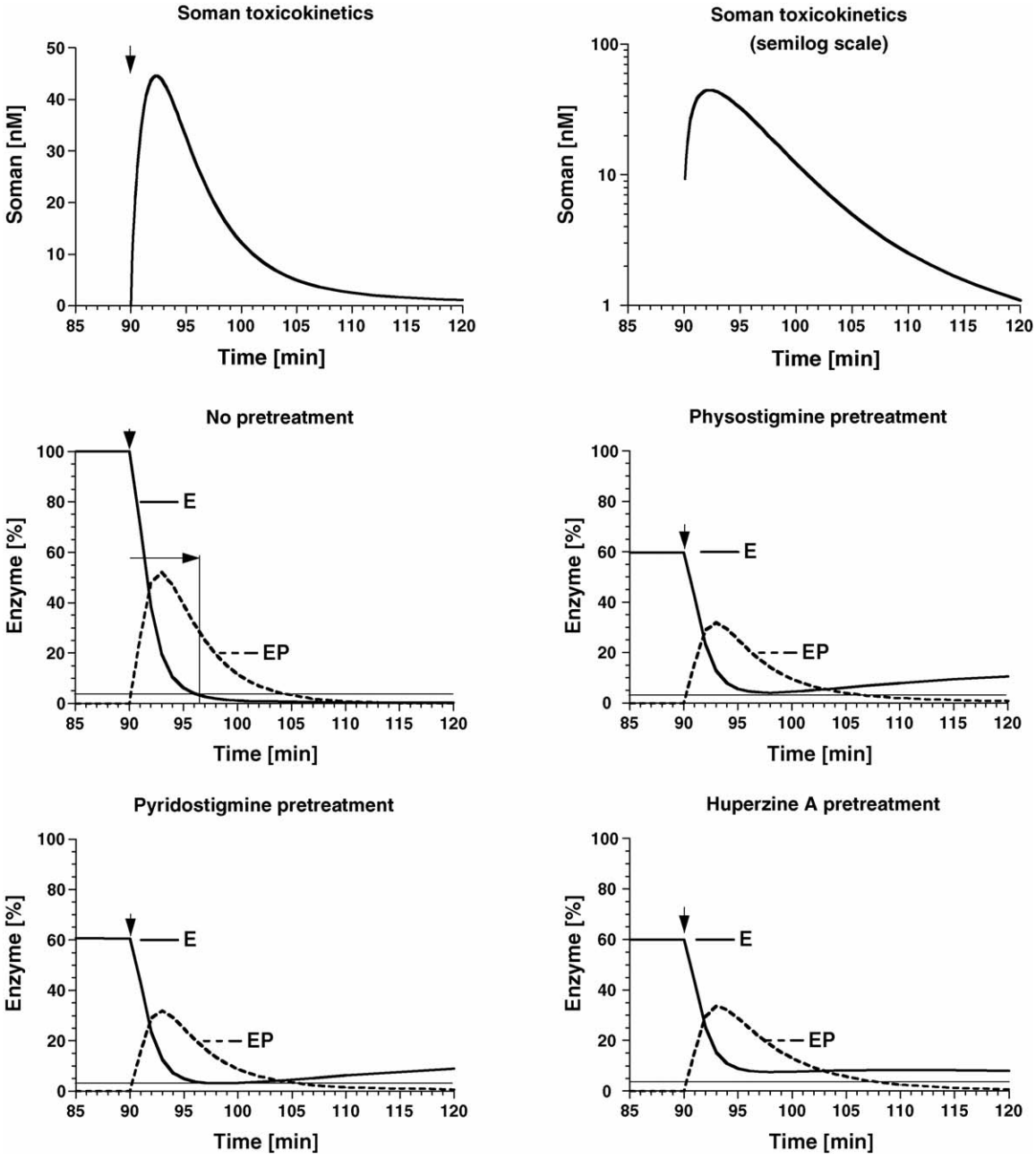

Fig. 14 – Influence of various pretreatment regimes on AChE following soman challenge: E (solid line), active enzyme; EP (dotted line), phosphonylated, unaged enzyme presented in an enlarged scale. Following pretreatment with the reversible inhibitor, soman was added after 90 min (arrow) at the simulated concentration shown in the left upper panel. The line drawn through 3% residual activity may indicate the minimal essential level of AChE. The right-handed arrow in the left middle panel indicates the time remaining until this minimal level is reached.

sufficient concentration. This simulation experiment shows that the quickly dissociating huperzine A may be superior over the carbamates in the case of a quickly acting 'hit-and-run poison', but may be of disadvantage when the agent is present for longer times.

The arbitrarily drawn line at 3% residual activity in Fig. 14 describes the 'minimal essential level of AChE', which deserves comment. In the rat, minimal levels of AChE for the maintenance of normal neuromuscular function were calculated to range between 1 and 10% of normal [14,36–38]. Based on a theoretical model that considered the contribution of carboxylesterase in protecting rats against organophosphorus poisoning, 7.5% of the initial level was found a reasonable estimate for the minimum amount of AChE required for survival [39]. For the brain, it has been suggested that 2% of normal AChE activity is the minimal essential level [40]. Conceivably, the minimal essential level may depend on the absolute activity rather than on the relative amount

expressed as percentage. Hence, this level may vary from species to species and among the vital organs. For the sake of demonstration, we chose a level of 3% of normal as a minimal essential level to provide the 'proof of principle'. Similar considerations had already lead Green to his hypothesis [28,41].

Given that such a level may be compatible with survival, severe incapacitation may thwart any useful function. In such a case, administration of further drugs by another person is mandatory. Reactivating oximes are probably of limited value since the time frame for reactivation is utmost narrow. Looking at Fig. 14 shows that under these conditions reactivating oximes such as HI 6 or HLö 7 [42–46] should reach effective systemic concentrations within 10 min after massive exposure. Otherwise aging prevents any significant reactivation in case of soman poisoning. Experiments are in progress to foster these predictions experimentally.

In conclusion, the experiments with the dynamic model have shown that pretreatment with a reversible inhibitor can enhance the residual AChE activity during a limited period of time when both a short-acting and an irreversible inhibitor are present. The effectiveness of the short-acting inhibitors varies in a systematic way: quick spontaneous reactivation is of advantage when a rapidly acting and rapidly disappearing irreversible inhibitor is involved. With slowly disappearing irreversible inhibitors, rapid spontaneous reactivation is probably of disadvantage. We do not think that a short-acting inhibitor will be found that covers a broad spectrum of irreversible inhibitors equally well.

Acknowledgement

The authors are grateful to Prof. B. Fichtl, Walther-Straub-Institute, for help with the mathematics and valuable suggestions.

REFERENCES

[1] Macilwain C. Study proves Iraq used nerve gas. Nature 1993;363:3.
[2] Nagao M, Takatori T, Matsuda Y, Nakajima M, Iwase H, Iwadate K. Definitive evidence for the acute sarin poisoning diagnosis in the Tokyo subway. Toxicol Appl Pharmacol 1997;144:198–203.
[3] Sidell F. Nerve agents. In: Sidell F, Takafuji ET, Franz DR, editors. Medical aspects of chemical and biological warfare. Washington: Walter Reed Army Medical Center; 1997. p. 130–79.
[4] Fleisher JH, Harris LW. Dealkylation as a mechanism for aging of cholinesterase after poisoning with pinacolyl methylphosphonofluoridate. Biochem Pharmacol 1965;14:641–50.
[5] Shafferman A, Ordentlich A, Barak D, Stein D, Ariel N, Velan B. Aging of phosphylated human acetylcholinesterase: catalytic processes mediated by aromatic and polar residues of the active centre. Biochem J 1996;318:833–40.
[6] Saxena A, Doctor BP, Maxwell DM, Lenz DE, Radic Z, Taylor P. The role of glutamate-199 in the aging of cholinesterase. Biochem Biophys Res Commun 1993;197:343–9.
[7] Talbot BG, Anderson DR, Harris LW, Yarbrough LW, Lennox WJ. A comparison of in vivo and in vitro rates of ageing of soman-inhibited erythrocyte anticholinesterase in different animal species. Drug Chem Toxicol 1988;11:289–305.
[8] Clement JG, Bailey DG, Madill HD, Tran LT, Spence JD. The acetylcholinesterase oxime reactivator HI-6 in man: pharmacokinetics and tolerability in combination with atropine. Biopharm Drug Disposit 1995;16:415–25.
[9] Lundy PM, Hill I, Lecavalier P, Hamilton MG, Vair C, Davidson C, et al. The pharmacokinetics and pharmacodynamics of two HI-6 salts in swine and efficacy in the treatment of GF and soman poisoning. Toxicology 2005;208:399–409.
[10] Koster R. Synergisms and antagonisms between physostigmine and di-isopropyl fluorophosphate in cats. J Pharmacol Exp Ther 1946;88:39–46.
[11] Koelle G. Protection of cholinesterase against irreversible inactivation by di-isopropyl fluorophosphate in vitro. J Pharmacol Exp Ther 1946;88:232–7.
[12] Berry WK, Davies DR. The use of carbamates and atropine in the protection of animals against poisoning by 1,2,2-trimethylpropyl methylphosphonofluoridate. Biochem Pharmacol 1970;19:927–34.
[13] Gordon JJ, Leadbeater L, Maidment MP. The protection of animals against organophosphate poisoning by pretreatment with a carbamate. Toxicol Appl Pharmacol 1978;43:207–16.
[14] Dirnhuber P, French MC, Green DM, Leadbeater L, Stratton JA. The protection of primates against soman poisoning by pretreatment with pyridostigmine. J Pharm Pharmacol 1979;31:295–9.
[15] Heyl WC, Harris LW, Stitcher DL. Effects of carbamates on whole blood cholinesterase activity: chemical protection against soman. Drug Chem Toxicol 1980;3:319–32.
[16] Lallement G, Baille V, Baubichon D, Carpentier P, Collombet JM, Filliat P, et al. Review of the value of huperzine as pretreatment of organophosphate poisoning. Neurotoxicology 2002;23:1–5.
[17] Gordon RK, Haigh JR, Garcia GE, Feaster SR, Riel MA, Lenz DE, et al. Oral administration of pyridostigmine bromide and huperzine A protects human whole blood cholinesterases from ex vivo exposure to soman. Chem Biol Interact 2005;157–158:139–46.
[18] Lennox WJ, Harris LW, Talbot BG, Anderson DR. Relationship between reversible acetylcholinesterase inhibition and efficacy against soman lethality. Life Sci 1985;37:793–8.
[19] Leadbeater L, Inns RH, Rylands JM. Treatment of poisoning by soman. Fundam Appl Toxicol 1985;5:S225–31.
[20] Maxwell DM, Brecht KM, Lenz DE, O'Neill BL. Effect of carboxylesterase inhibition on carbamate protection against soman toxicity. J Pharmacol Exp Ther 1988;246:986–91.
[21] Li B, Sedlacek M, Manoharan I, Boopathy R, Duysen EG, Masson P, et al. Butyrylcholinesterase, paraoxonase, and albumin esterase, but not carboxylesterase, are present in human plasma. Biochem Pharmacol 2005;70:1673–84.
[22] Koplovitz I, Harris LW, Anderson DR, Lennox WJ, Stewart JR. Reduction by pyridostigmine pretreatment of the efficacy of atropine and 2-PAM treatment of sarin and VX poisoning in rodents. Fundam Appl Toxicol 1992;18:102–6.
[23] von Bredow JD, Adams NL, Groff WA, Vick JA. Effectiveness of oral pyridostigmine pretreatment and cholinolytic-oxime therapy against soman intoxication in nonhuman primates. Fundam Appl Toxicol 1991;17:761–70.
[24] Aldridge WN, Reiner E. Enzyme inhibitors as substrates. In: Interactions of esterases with esters of organophosphorus and carbamic acids. Amsterdam: North-Holland Publ. Co.; 1972.

[25] Deshpande SS, Viana GB, Kauffman FC, Rickett DL, Albuquerque EX. Effectiveness of physostigmine as a pretreatment drug for protection of rats from organophosphate poisoning. Fundam Appl Toxicol 1986;6:566–77.
[26] Worek F, Szinicz L, Eyer P, Thiermann H. Evaluation of oxime efficacy in nerve agent poisoning: development of a kinetic-based dynamic model. Toxicol Appl Pharmacol 2005;209:193–202.
[27] Kozikowski AP, Xia Y, Reddy ER, Tückmantel W, Hanin I, Tang XC. Synthesis of huperzine A and its analogues and their anticholinesterase activity. J Org Chem 1991;56:4636–45.
[28] Green AL. A theoretical kinetic analysis of the protective action exerted by eserine and other carbamate anticholinesterases against poisoning by organophosphorus compounds. Biochem Pharmacol 1983;32:1712–22.
[29] Worek F, Bäcker M, Thiermann H, Szinicz L, Mast U, Klimmek R, et al. Reappraisal of indications and limitations of oxime therapy in organophosphate poisoning. Hum Exp Toxicol 1997;16:466–72.
[30] Eyer F, Eyer P. Enzyme-based assay for quantification of paraoxon in blood of parathion poisoned patients. Hum Exp Toxicol 1998;17:645–51.
[31] Hart GJ, O'Brien RD. Recording spectrophotometric method for determination of dissociation and phosphorylation constants for the inhibition of acetylcholinesterase by organophosphates in the presence of substrate. Biochemistry 1973;12:2940–5.
[32] Mast U. Reactivation of erythrocyte acetylcholinesterase by oximes. Establishment of enzyme kinetic constants and their implications in therapy of organophophate poisoning. Thesis, München; 1997.
[33] Cook JE, Kolka MA, Wenger CB. Chronic pyridostigmine bromide administration: side effects among soldiers working in a desert environment. Military Med 1992;157:250–4.
[34] Dunn MA, Sidell FR. Progress in medical defense against nerve agents. J Am Med Assoc 1989;262:649–52.
[35] Benschop HP, de Jong LPA. Toxicokinetics of nerve agents. In: Somani SM, Romano JA, editors. Chemical warfare agents: toxicity at low levels. Boca Raton: CRC Press; 2001. p. 25–81.
[36] Barnes JM, Duff JI. The role of cholinesterase at the myoneural junction. Brit J Pharmacol 1953;8:334–9.
[37] Meeter E, Wolthuis OL. The spontaneous recovery of respiration and neuromuscular transmission in the rat after anticholinesterase poisoning. Eur J Pharmacol 1968;2:377–86.
[38] Hobbiger F. Pharmacology of anticholinesterase drugs. In: Zaimis E, editors. The neuromuscular junction. Handb Exp Pharmacol. Berlin Heidelberg New York: Springer, 1976;42:487–581.
[39] Sweeney RE, Maxwell DM. A theoretical model of the competition between hydrolase and carboxylesterase in protection against organophosphorus poisoning. Math Biosci 1999;160:175–90.
[40] Kewitz H, Nachmansohn D. A specific antidote against lethal alkylphosphate intoxication. IV. Effects in brain. Arch Biochem Biophys 1957;66:271–83.
[41] Green AL. The kinetic basis of organophosphate poisoning and its treatment. Biochem Pharmacol 1958;1:115–28.
[42] Oldiges H, Schoene K. Pyridinium- und Imidazoliumsalze als Antidote gegenüber Soman- und Paraoxonvergiftungen bei Mäusen. Arch Toxicol 1970;26:293–305.
[43] de Jong LPA, Wolring GZ. Reactivation of acetylcholinesterase inhibited by 1,2,2′-trimethylpropyl methylphosphonofluoridate (soman) with HI-6 and related oximes. Biochem Pharmacol 1980;29:2379–87.
[44] Hamilton MG, Lundy PM. HI-6 therapy of soman and tabun poisoning in primates and rodents. Arch Toxicol 1989;63:144–9.
[45] Eyer P, Hagedorn I, Klimmek R, Lippstreu P, Löffler M, Oldiges H, et al. HLö 7 dimethanesulfonate, a potent bispyridinium-dioxime against anticholinesterases. Arch Toxicol 1992;66:603–21.
[46] Busker RW, Zijlstra JJ, Philippens IHCHM, Groen B, Melchers BPC. Comparison of the efficacy of single or repeated HI 6 treatment following soman poisoning in guinea-pigs and marmoset monkeys. Toxicology 1996;112:183–94.
[47] Harris LW, Heyl WC, Stitcher DL, Broomfield CA. Effects of 1,1′-oxydimethylene-bis-(4-tertbutylpyridinium chloride) (SAD-128) and decamethonium on reactivation of soman- and sarin-inhibited cholinesterase by oximes. Biochem Pharmacol 1978;27:757–61.
[48] de Jong LPA, Wolring GZ. Stereospecific reactivation by some Hagedorn-oximes of acetylcholinesterases from various species including man, inhibited by soman. Biochem Pharmacol 1984;33:1119–25.